J Nanopart Res (2016) 18:79
DOI 10.1007/s11051-016-3378-1

RESEARCH PAPER

Improvement of kinetics, yield, and colloidal stability of biogenic gold nanoparticles using living cells of *Euglena gracilis* microalga

Si Amar Dahoumane · Claude Yéprémian · Chakib Djédiat · Alain Couté · Fernand Fiévet · Thibaud Coradin · Roberta Brayner

Received: 23 September 2015 / Accepted: 23 February 2016 / Published online: 10 March 2016

Abstract Recent years have witnessed a boom in the biosynthesis of a large variety of nanomaterials using different biological resources among which algae-based entities have been gaining much more attention within the community of material scientists worldwide. In our previously published findings, we explored some factors that governed the biofabrication of gold nanoparticles using living cultures of microalgae, such as the utilized microalgal genera, the phylum they belong to, and the impact of tetrachloroauric acid concentrations on the ability of these strains to perform the biosynthesis of gold nanoparticles once in contact with these cations. As a follow-up, we present in this paper an improvement of the features of bioproduced gold colloids using living cells of *Euglena gracilis* microalga when this species is grown under either mixotrophic or autotrophic conditions, i.e., exposed to light and grown in an organic carbon-enriched culture medium versus under autotrophic conditions. As an outcome to this alteration, the growth rate of this photosynthetic microorganism is multiplied 7–8 times when grown under mixotrophic conditions compared to autotrophic ones. Therefore, the yield, the kinetics, and the colloidal stability of the biosynthesized gold nanoparticles are dramatically enhanced. Moreover, the shape and the size of the as-produced nano-objects via this biological method are affected. In addition to round-shaped gold nanoparticles, particular shapes, such as triangles and hexagons, appear. These findings add up to the amassed knowledge toward the design of photobioreactors for the scalable and sustainable production of interesting nanomaterials.

Keywords Biotechnology · *Euglena gracilis* · Gold nanoparticles · Biosynthesis · Colloidal stability · Kinetics · Yield

S. A. Dahoumane · F. Fiévet · R. Brayner
Sorbonne Paris Cité, Interfaces, Traitements, Organisation et Dynamique des Systèmes (ITODYS), UMR 7086, CNRS, Paris-Diderot University, 15 rue Jean de Baïf, 75205 Paris Cedex 13, France
e-mail: roberta.brayner@univ-paris-diderot.fr

S. A. Dahoumane (✉)
School of Life Sciences and Biotechnology, Hacienda San José, Yachay Tech University, San Miguel de Urcuquí, Ecuador
e-mail: sa.dahoumane@gmail.com

C. Yéprémian · C. Djédiat · A. Couté
Département RDDM, UMR 7245, Unité MCAM, Muséum National d'Histoire Naturelle, 57 rue Cuvier, case 39, 57 rue Cuvier, 75005 Paris, France

T. Coradin
UPMC—Paris 06, CNRS, Chimie de la Matière Condensée de Paris, Collège de France, 11 place Marcellin Berthelot, 75005 Paris, France
e-mail: thibaud.coradin@upmc.fr

Introduction

Nanomaterial biosynthesis refers to the use of biological resources, such as bacteria, fungi, plants, and biomolecules, as biocatalysts for the production of

inorganic nano-structured objects (Castro et al. 2014; Jeffryes et al. 2015; Klaus-Joerger et al. 2001; Pantidos and Horsfall 2014). Generally, these biocatalysts act, at the same time, as the reducing and capping agents. After a slow start, the utilization of algal resources for the bioproduction of various nanomaterials has witnessed an outstanding boom. The paper by Liu et al. (2005) was the first paper to ever report on the biosynthesis of gold nanoparticles using aqueous extracts of the brown macroalga, or seaweed, *Sargassum* sp. (Liu et al. 2005). This pioneering work demonstrated that, by tuning the experimental parameters, such as the pH, the reaction time, the temperature, and the amount of used biomass, it is possible to tailor the features of the so-produced gold nanoparticles and obtain, under certain conditions, triangular or hexagonal nanoplates.

Several methodologies using algae-based bioactive materials have been devised for the biosynthesis of a large range of nanomaterials starting from the corresponding salts. For instance, the algal biomass can be under the form of an aqueous extract or broth, collected intact cells of microalgae which are then suspended in double-distilled water (ddH_2O), living cells of microalgae maintained under their normal culturing conditions, or purified proteins from algal species. The aqueous extract is generally collected from macroalgae, especially brown, red, and green ones, and used as a mediator for the biosynthesis of nanomaterials made of gold (Castro et al. 2013; Mata et al. 2009; Rajeshkumar et al. 2013; Sharma et al. 2014), silver (Govindaraju et al. 2009; Kannan et al. 2013; Kumar et al. 2013, 2012), palladium (Momeni and Nabipour 2015), iron oxide (Mahdavi et al. 2013), and zinc oxide (Azizi et al. 2014; Nagarajan and Kuppusamy 2013; Pandimurugan and Thambidurai 2014). Collected intact cells of microalgae are exploited in the biosynthesis of gold (Chakraborty et al. 2009; Lengke et al. 2006; Parial et al. 2012; Senapati et al. 2012), silver (Barwal et al. 2011; Jena et al. 2014; Lengke et al. 2007; Li et al. 2015; Mahdieh et al. 2012; Patel et al. 2015), platinum (Lengke et al. 2006), palladium (Lengke et al. 2007), copper oxide (Rahman et al. 2009), and iron-based (Subramaniyam et al. 2015) nano-objects. Purified algal proteins are exploited in the fabrication of nanoparticles made of gold (Xie et al. 2007), silver (Xie et al. 2007), and silver–gold bimetallic nanoparticles (Govindaraju et al. 2008). Furthermore, the pigment C-phycoerythrin, extracted from a marine cyanobacterium, is utilized for the production of CdS nanoparticles (MubarakAli et al. 2012).

The use of living cells of microalgae, more specifically cyanobacteria, maintained under their normal culturing conditions, for the biosynthesis of different nanomaterials was first reported by Brayner and colleagues (Brayner et al. 2007). This simple and 1-step process consists in, first, growing cells in a flask containing their culture media for a certain amount of time and, then, challenging the cells by aqueous solutions of metallic salts. As a result, the living cells act as green nanofactories inside which the production of the targeted nanomaterials occurs. Although the mechanism underlying this phenomenon has yet to be fully investigated, a few papers provide with meaningful hints (Dahoumane et al. 2014b; Jeffryes et al. 2015; Rösken et al. 2014). The novelty of this methodology lies in the advantage taken from the enzymatic machinery of microalgae, either they are unicellular or filamentous, to accomplish the production of the desired nanomaterials while the cells are maintained under their habitual culturing conditions offering hence the possibility for the design of bioreactors (Satapathy et al. 2014). Although in its early infancy, devising algae-based photobioreactors for the biosynthesis of various and valuable nanomaterials should witness tremendous developments in the near future owing to the ease of microalgae culturing and the various nanomaterials reported to date having been produced through this expanding eco-friendly route (vide infra).

So far, several studies have described the biosynthesis of a myriad of nanomaterials using living cultures of microalgae belonging to five algal divisions. For instance, gold nanoparticles can be synthesized using living cultures of *Charophyta Klebsormidium flaccidum* and *Cosmarium impressulum* (Dahoumane et al. 2012a, b); *Chlorophyta Kirchneriella lunaris* (Dahoumane et al. 2014b), *Pseudokirchneriella subcapitata* (Lahr and Vikesland 2014), and *Chlorella vulgaris* (Luangpipat et al. 2011); *Cyanophyta Anabaena* sp. (Rösken et al. 2014), *Synechocystis* sp. (Focsan et al. 2011), *Anabaena flos-aquae*, *Calothrix pulvinata* and *Leptolyngbya foveolarum* used also for the biosynthesis of Pt, Pd, and Ag nanoparticles (Brayner et al. 2007); diatoms *Eolimna minima* (Feurtet-Mazel et al. 2015), *Diadesmis gallica* and *Navicula atomus* (Schröfel

et al. 2011); and *Euglenozoa Euglena gracilis* (Dahoumane et al. 2012a). In a similar manner, silver nanoparticles can be produced through the use of living cultures of *Chlorella vulgaris* (Mohseniazar et al. 2011) and *Pseudochlorella kessleri* (Kaduková et al. 2014); silver–gold bimetallic alloy nanoparticles of well-controlled composition using living cultures of *Chlorophyta Chlamydomonas reinhardtii* (Dahoumane et al. 2014a); and iron oxide nanomaterials using *Charophyta K. flaccidum* (Brayner et al. 2009), *Euglenozoa E. gracilis* (Brayner et al. 2012), and *Cyanophyta A. flos-aquae* (Dahoumane et al. 2010).

In this paper, we report on the improvement of the kinetics and the yield of biogenic gold nanoparticles using *E. gracilis* living cultures after the addition of tetrachloroauric acid aqueous solutions into the cultures by the mean of culture media switching from mineral medium—organic carbon free, to lactate medium—a source of organic carbon. This change affects the rate of growth of *E. gracilis* and its viability, which, in turn, affect the features of gold biosynthesis, i.e., the kinetics, the yield, and the characteristics of the so-fabricated gold nano-objects via *E. gracilis*-mediated route, namely the size, the shape, and the colloidal stability.

Materials and methods

Euglena gracilis presentation and culturing conditions

Euglena gracilis (ALCP#217) comes from the Muséum National d'Histoire Naturelle (Paris, France) Culture Collection. It is a unicellular motile protist belonging to the algal phylum of *Euglenozoa*, provided, in addition to a functional photosynthetic machinery, with the ability to perform phagocytosis. It can be cultured in a carbon-free, mineral (M) medium, i.e., under autotrophic conditions where cells perform only photosynthesis, or under mixotrophic conditions where cells are grown in organic carbon-rich media, such as lactate (L) medium, and exposed to light so the cells can rely on both photosynthesis and phagocytosis to grow. Both media, M and L, derive from bold basal (BB) medium (Stein 1973). For the optimum growth of *E. gracilis*, the pH is brought to 3.6 by addition of HCl 1 N, in the case of mineral (M) medium, and of a mixture of lactic acid/sodium lactate, in the case of lactate (L) medium. Finally, the media are autoclaved at 121 °C for 20 min and stored at 4 °C.

Starting from a stock culture of *E. gracilis* grown in L medium, the culture was transferred (10 % (v/v) of inoculum) into the culture medium. In duplicate, 10 mL of the stock culture were added into a sterile 250 mL flask containing 90 mL of L medium and let to grow for 2 weeks before use, in an incubator with a photoperiod of 16-h light/8-h dark, at a controlled temperature of 20.0 ± 1.0 °C and luminosity (70–100 µmol m^{-2} s^{-1} PPF) under ambient CO_2 conditions. A similar procedure was followed for the launch of *E. gracilis* grown in M medium.

Biosynthesis of Au-NPs using living cells of *Euglena gracilis*

The biosynthesis of gold nanoparticles (Au-NPs) using living cells of *E. gracilis* cultured in L (*Eg*L) and M (*Eg*M) media was carried out as described previously (Dahoumane et al. 2012a). Typically, aqueous solutions of tetrachloroauric acid ($HAuCl_4$) were added into 2-week-old cultures. For *Eg*L 1 and *Eg*M 1, a final Au(III) concentration of 10^{-3} M was reached starting from an initial aqueous solution of $HAuCl_4$ at 10^{-2} M; for *Eg*L 2, a final Au(III) concentration of 10^{-4} M was reached starting from an initial aqueous solution of $HAuCl_4$ at 10^{-3} M. After $HAuCl_4$ introduction, the flasks containing the cultures were put back into the incubator and gently hand-shaken twice a day.

Characterization of *Euglena gracilis* cells and Au-NPs

Cell growth and viability

The cell viability of *Eg*L 1, *Eg*M 1, and *Eg*L 2 was monitored by measuring the absorbance of chlorophyll a at different times before and after $HAuCl_4$ addition. This photosynthetic pigment is extracted from 1 mL of *E. gracilis* cultures in 9 mL of acetone, according to an experimental protocol published by Ninfa et al. (2010). After 1 min of vortex, the mixture is warmed up to 37 °C for 3 min and then centrifuged. The obtained supernatant is used to monitor, throughout the experiment, the evolution of chlorophyll a main

peak absorbance, centered at 663 nm, by UV–Vis spectroscopy using a Cary 5E spectrophotometer.

Au-NP absorbance

The evolution over time of the surface plasmon resonance (SPR) band intensity of the as-produced gold colloids, after the addition of gold salt solutions into the three cultures of *E. gracilis*, was monitored by UV–Vis spectroscopy using a Cary 5E spectrophotometer. ~2 mL of the colloids were scanned between 400 and 800 nm, at different times.

Optical microscopy

Optical microscopy was performed with a Zeiss Primo Star microscope.

TEM

Transmission electron microscopy (TEM) micrographs of the released Au-NPs were obtained using a JEOL JEM 100CX II UHR operating at 100 kV. Droplets of the supernatant taken from *Eg*L 1 containing Au-NPs were cast onto formvar-coated copper grids, and the water was allowed to evaporate.

SEM-FEG

Scanning electron microscopy using field emission gun (SEM-FEG) was performed using Zeiss Supra 40 operating at 20 kV. Secondary electron detector was used. Prior to observation, the samples were fixed using glutaraldehyde, dehydrated in acetone, and dried with a critical point dryer BAL-TEC CPD 030 with liquid CO_2, critical point 31 °C—73.8 bar.

Results and discussion

Cell growth and viability

To assess the rate of growth of *E. gracilis* when cultured in lactate (L) medium, Fig. 1 presents the absorbance of the photosynthetic pigments, i.e., chlorophylls a and c and carotenoids, extracted from 2-week-old cultures. Each pigment has several com-

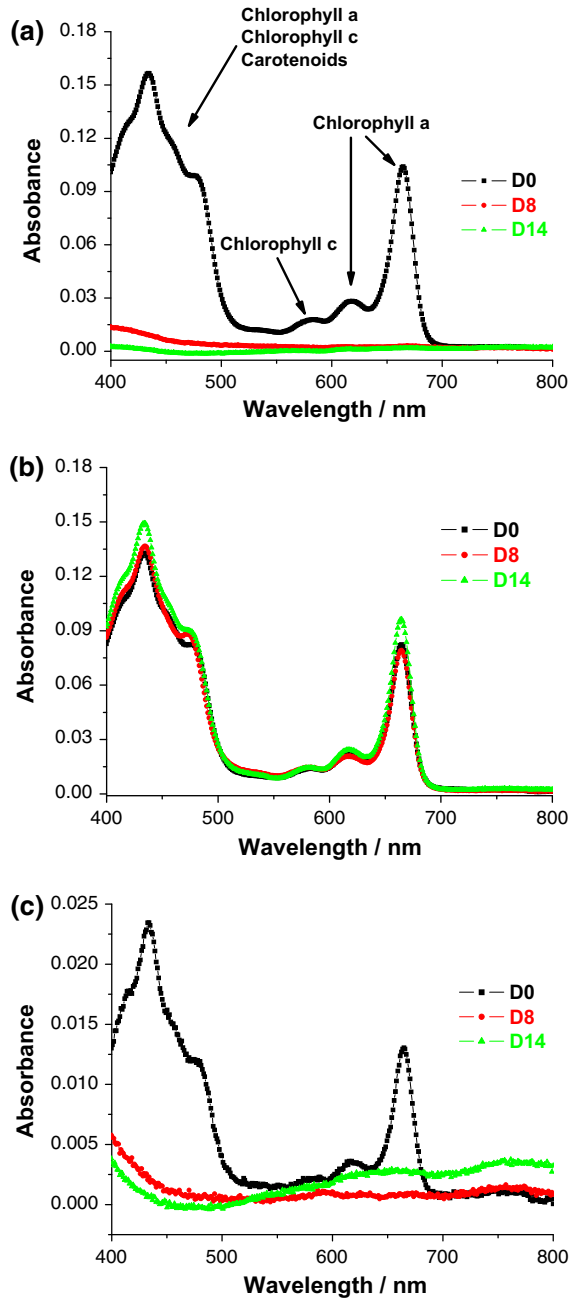

Fig. 1 Evolution of the absorbance of acetone-extracted photosynthetic pigments of 2-week-old *E. gracilis* grown in L (*Eg*L) (**a**, **b**) and in M (*Eg*M) (**c**) culture media before (D0 spectrum) and after the addition of aqueous $HAuCl_4$ solutions, 8 and 14 days later (D8 and D14 spectra, respectively) at 10^{-3} M (**a**, **c**) and 10^{-4} M (**b**). The *black arrows* in **a** (D0 spectrum) indicate the components of these pigments, i.e., chlorophylls *a* and *c* and carotenoids

ponents, indicated with black arrows in Fig. 1a—D0 spectrum, overlapping with those of the other pigments. The absorbance of the chlorophyll a most intense band, located at ~663 nm, is taken as an indicator of cell growth and viability. After 2 weeks of growth and prior to $HAuCl_4$ introduction into the *Eg*L cultures, the intensities were ~0.10 and ~0.08 for flasks a and b (Fig. 1a, b—D0 spectrum, respectively). If the 10-fold dilution factor is taken into account, this makes the chlorophyll a absorbance at ~1.00 and ~0.80 for the same flasks, respectively. These values have to be compared with the absorbance of chlorophyll a of the same species when cultured in mineral (M) medium. As depicted in Fig. 1c—D0 spectrum, the 2-week-old flask of *E. gracilis*, grown in M medium, displays an absorbance of ~0.012 for the chlorophyll a, ~0.12 if the dilution factor is taken into account (Dahoumane et al. 2012a, 2014b). This means that *E. gracilis* has a rate of growth 7–8 times faster when grown in L medium compared to M medium. In other words, L medium contributes to the greater part of the growth versus photosynthesis. This fast rate of growth has a direct consequence on the ability of the cultures to handle the introduced tetrachloroauric cations (vide infra).

The addition of tetrachloroauric acid aqueous solutions into the cultures triggered two distinct behaviors of *E. gracilis* cultures regarding the viability. At 10^{-3} M, the chlorophyll a signal totally disappeared 8 days after (Fig. 1a, c—D8 spectrum). Two weeks later (Fig. 1a, c—D14 spectrum), no sign of recovery was recorded. Unlike the two previous cases, chlorophyll a maintained its amount within the *Eg*L culture 8 days after Au(III) addition at 10^{-4} M (Fig. 1b—D0 and D8 spectra) and witnessed a slight increase 6 days later (Fig. 1b—D14 spectrum). In other words, the culture underwent a partial damage during the first week caused by the toxicity of Au(III) cations but soon recovered by reaching its initial growth level and then continued multiplying. These findings confirm our previously reported results, i.e., in all cases, 10^{-3} M of Au(III) is a lethal dose for microalgae cells, while 10^{-4} M of Au(III) can, in some cases, inhibit the cell growth for a short while but without any significant incidence on the cell growth at a long course (Dahoumane et al. 2012a, 2014b).

Notably, the use of acetone as the chlorophyll a extracting agent led to the disappearance, in all spectra, of the SPR band due to the absorbance of Au-NPs. So far, this band remained visible when chlorophyll a absorbance was measured in the case of only *K. lunaris* and *C. reinhardtii* used as nanofactories for the biosynthesis of Au-NPs (Dahoumane et al. 2014b), and Au-, Ag-, and Ag/Au bimetallic alloy NPs (Dahoumane et al. 2014a), respectively. The persistence of the SPR band in the case of these two green microalgae species is due to the protection of the as-synthesized metallic NPs ensured by the adsorption of the cell-produced mucilage onto the NP surface through a strong interaction. As *E. gracilis* is not known to produce any exopolysaccharides, the so-fabricated nanoparticles might not offer any stability. However, when grown in L medium, the lactate may act as the capping agent, offering therefore a relatively average stability that could not withstand the action of acetone.

Macroscopic aspect of *Euglena gracilis* cultures

The macroscopic aspect of *E. gracilis* cultures grown in L medium is in good agreement with the recorded spectra of the chlorophyll a, i.e., the more intense is the absorbance of chlorophyll a, the darker green is the color of the flasks containing the cultures. In fact, as depicted in Fig. 2a-1, b-1, the 2-week-old cultures of *E. gracilis* grown in L medium (a-1 and b-1 photographs) appear completely dark green compared to when grown in M medium which presents a lighter green color (Fig. 2c-1 photograph). This is due to the fact that *E. gracilis* in L medium feeds predominantly directly from its nourishing medium in addition to carrying out photosynthesis.

One day after the addition of the chloroauric cations into the flasks at 10^{-3} M, the color shifts from dark green into dark purple in the case of *Eg*L 1 (Fig. 2a-2 photograph) and from light green into brown in the case of *Eg*M 1 (Fig. 2c-2 photograph), respectively. This color change evidences the transformation of cationic gold into its zero-valent counterpart. However, no change is noticed in the case of *Eg*L 2 ($[Au^{3+}] = 10^{-4}$ M) where the culture remains dark green (Fig. 2b-2 photograph).

Photonic imaging of *Euglena gracilis* cells

To check whether the production of Au-NPs by *E. gracilis* cultured in L medium is an intracellular process, similarly to when cultured in M medium (Dahoumane et al. 2012a), and having in mind that

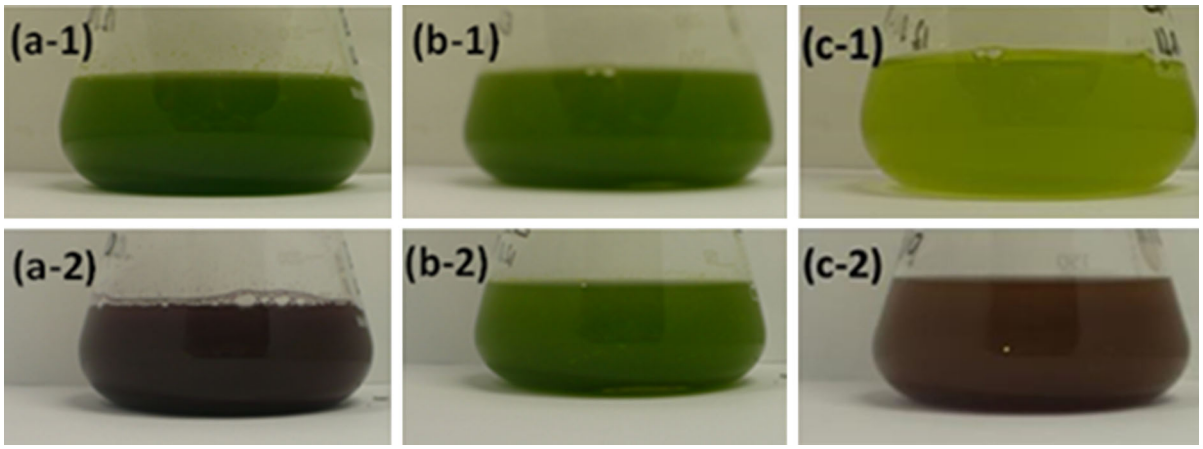

Fig. 2 Evolution of the macroscopic aspect of *E. gracilis* cultures grown in L (*Eg*L) (**a**, **b**) and M (*Eg*M) media (**c**) before (**a**-1, **b**-1, **c**-1) and one day (D + 1) after the addition of tetrachloroauric acid aqueous solutions ($HAuCl_4$) at 10^{-3} M (**a**-2, **c**-2) and 10^{-4} M (**b**-2)

lactic acid was reported to promote the synthesis of gold nanoparticles by acting as the reducing agent under boiling conditions (Yin et al. 2010), we decided to pick up a small volume of *Eg*L 1 culture medium after gold cations were added at a concentration of 10^{-3} M and imaged the sample using an optical microscope. As shown in Fig. 3, all compartments of *E. gracilis* cells became purple, proving therefore that the cells internalized the introduced Au(III) and reduced them through an intracellular process into metallic gold (Au(0)) before releasing the as-generated Au-NPs into culture media, demonstrating thus that, for *E. gracilis*, the same 3-step intracellular process regarding Au-NP biosynthesis occurs in both culture media: (i) uptake of Au(III); (ii) reduction of Au(III) into Au(0), and subsequent Au-NP generation; and (iii) release of the as-produced Au-NPs into culture media. Moreover, the image highlights the well-known characteristic of *E. gracilis* regarding its ability to change steadily its shape and size. In fact, the three shown cells display different shapes and sizes; two of them are sticking one to another, while the third one is shown enveloped in a kind of a purple cloud. This last fact may be explained by two reasons: the cell lysis leading to the release of the intracellular components overloaded with intracellular Au-NPs due to the toxicity of these objects and/or the cell is erupting due to the applied pressure by the two glass slides used for imaging.

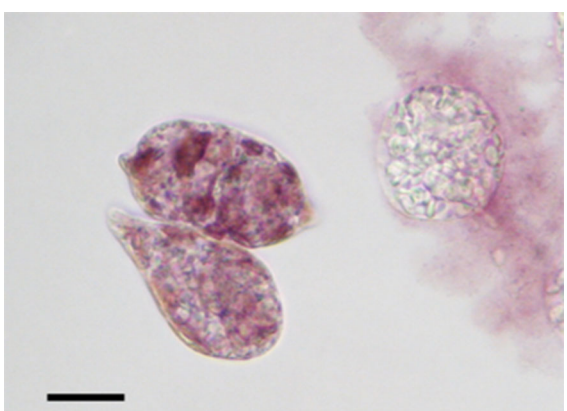

Fig. 3 Optical image of *E. gracilis* cells grown in L medium and challenged with 10^{-3} M of $HAuCl_4$ aqueous solution (*Eg*L 1 sample). Scale bar 10 μm

State of the surface of *Euglena gracilis*

The surface of *E. gracilis* cells, taken from *Eg*L 1 sample—cultured in L medium and challenged by 10^{-3} M of Au(III), was characterized using scanning electron microscopy using a field emission gun (SEM-FEG). Figure 4a displays a whole cell of *E. gracilis* with a preserved outer structure. At the top of the micrograph, the longest flagellum, indicated with the red arrow, can be distinguished easily at the cell apex. Moreover, the pellicle, made of strips spiraling around the cell, is also neatly visible. This pellicle ensures to *E. gracilis* its flexibility, i.e., perpetual changes in shape and size, and contractility making it motile. At this magnification, it is hard to distinguish any Au-NPs

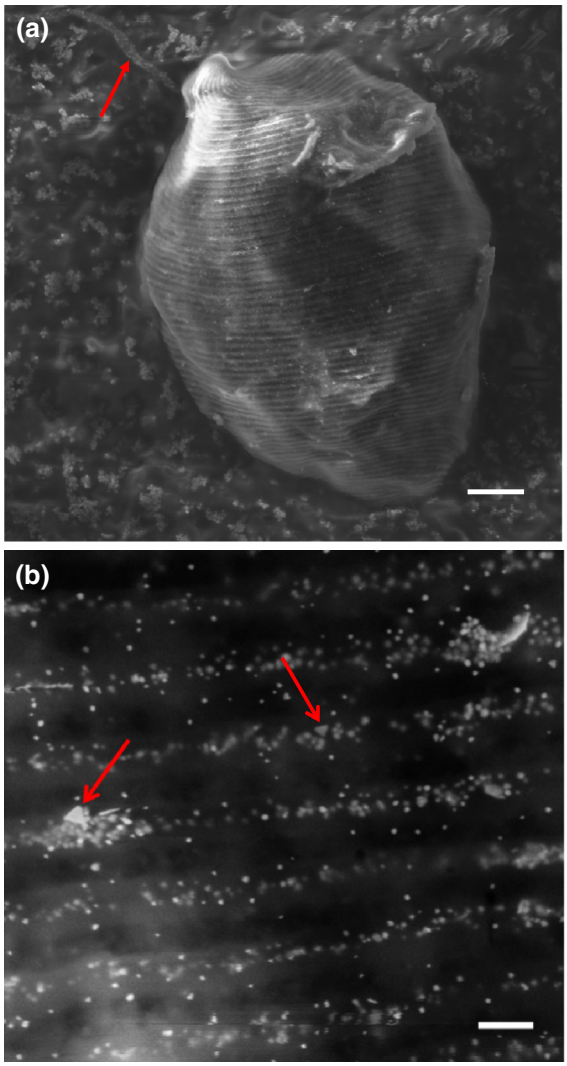

Fig. 4 SEM-FEG micrographs of **a** a whole cell of *E. gracilis* grown in L medium and challenged with Au(III) at 10^{-3} M (*Eg*L 1). *Red arrow* indicates the cell longest flagellum; and **b** a higher magnification of a part of the same cell. *Red arrows* indicate visible gold nanoparticles under the shape of a triangle on the surface of *E. gracilis*. Scale bar 2 μm (**a**) and 200 nm (**b**)

located at the surface of the cells. Besides depicting the well-preserved pellicle and the absence of any damage, higher magnification (Fig. 4b) on a part of the previous image shows spots with 3 level of brightness due to the presence of Au-NPs at 3 different compartments/depths: (i) the brightest spots are located on the cell surface; (ii) the palest ones are located within the cell in the shallow compartments; and (iii), with an in-between brightness, the nano-objects located under the cell surface and about to be released from the cells. These findings corroborate the intracellular formation of these nanoparticles which diffuse to the cell wall where they are released into culture media (Dahoumane et al. 2012a). A deeper look on the nanoparticles located on the surface of *E. gracilis* allows to notice that these Au-NPs seem to form a homogenous population sharing the same characteristics with a spherical shape and a narrow distribution in size. The presence of particular shapes, such as triangles and hexagons, indicated in red arrows in Fig. 4, is very scarce.

Shape and size of biogenic gold nanoparticles

Two weeks after the living cells of *E. gracilis* were challenged by tetrachloroauric acid at a concentration of 10^{-3} M (*Eg*L 1), a small volume of the supernatant was examined using a TEM in order to study the shape and the size of the released Au-NPs from the cells into

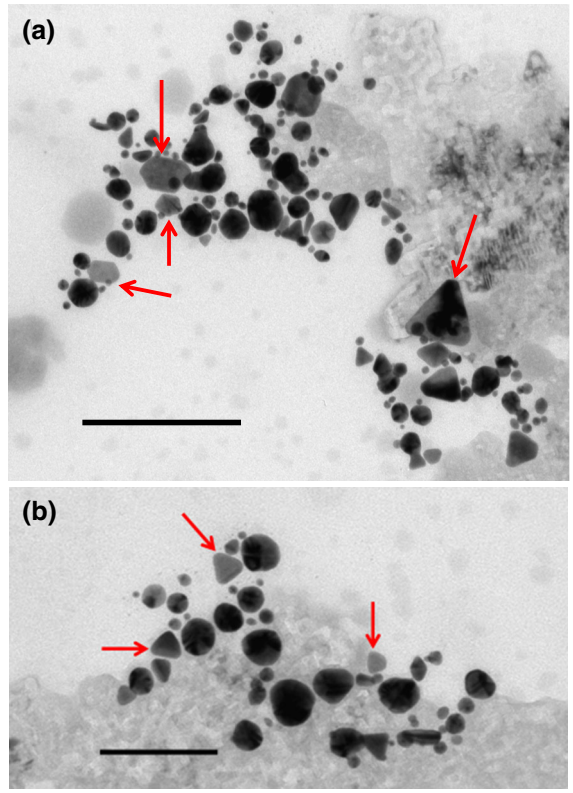

Fig. 5 TEM micrographs of released Au-NPs taken from the supernatant of *E. gracilis* grown in L medium (*Eg*L 1, $[Au^{3+}] = 10^{-3}$ M). *Red arrows* indicate some Au-NPs of particular shapes, such as triangles, pentagons, and hexagons. Scale bar 200 nm (**a**) and 100 nm (**b**)

the culture medium (Fig. 5). Overall, the nanoparticles look well-defined and well-dispersed and do not aggregate. Mainly, three major populations of Au-NPS can be easily distinguished: small round-shaped nanoparticles of less than 10 nm in diameter, big round-shaped nanoparticles of tens of nm in diameter, and nanoparticles under the shape of triangle, truncated triangles, pentagons, and hexagons, referred to with red arrows in Fig. 5a, b, whose dimensions vary from a few nanometers to tens of nanometers. In the absence of SEM micrographs, these TEM images cannot allow to state whether these particular shapes exhibit the same depth and could be coined as nanoplates or not. The first two sorts of Au-NPs are also visible when *E. gracilis* is grown in mineral medium (Dahoumane et al. 2012a, 2014b). However, the latter occurs only in the present case, i.e., in L medium, and is not seen when *E. gracilis* is grown in mineral (M) medium (*Eg*M) and challenged with gold cations either at 10^{-3} or 10^{-4} M (Dahoumane et al. 2012a, 2014b). Therefore, Au-NPs, under the shape of triangles, pentagons, and hexagons, could not be formed through an intracellular process. Indeed, the ultrastructure of several species of microalgae involved in the bioproduction of Au-NPs, including *E. gracilis* grown in M medium, does not show such shapes within the cells (Brayner et al. 2007; Dahoumane et al. 2012b). This fact is supported by the recent study by Li et al. who carried out the synthesis of Ag-NPs using two different strains of *Euglena* (Li et al. 2015). Moreover, a meticulous examination of the surface of *E. gracilis*, from our experiment, i.e., *Eg*L 1, using SEM-FEG, demonstrates that Au-NPs under these shapes are not visible either within the cells in the shallow compartments or just beneath the cell surface, and are very scarce on the surface of the cells (cf. Fig. 4). We think the apparition of Au-NPs under these shapes, i.e., triangles, truncated triangles, pentagons, and hexagons, may likely be due to the combination of two factors: the mass cell lysis, caused by the toxicity of Au(III) at 10^{-3} M, triggers the release of biomolecules from the cells; once in culture medium, these biomolecules can act along with lactate as reducing agents yielding to the extracellular biosynthesis of Au-NPs or alteration of the features of Au-NPs synthesized via an intracellular process, i.e., the shape and the size; finally, the lactate and the available released biomolecules from lysed cells, by adsorbing preferentially on certain facets of the growing nuclei and modifying their relative growth rates, may direct the shape of the Au-NPs leading therefore to the formation of these Au-NP particular shapes. The ability of lactate to reduce gold cations and direct the shape of the as-produced NPs was discussed in the paper by Yin et al. (2010).

Kinetics, yield, and colloidal stability

In order to compare the features of the as-produced gold nanoparticles, i.e., the kinetics, the yield, and the colloidal stability, between *Eg*L 1 ($[Au^{3+}] = 10^{-3}$ M), *Eg*L 2 ($[Au^{3+}] = 10^{-4}$ M), and *Eg*M 1 ($[Au^{3+}] = 10^{-3}$ M), the intensity of the SPR band, due to the presence of nano-gold within each sample, was recorded using UV–Vis spectroscopy at different times and the results are summed up in Fig. 6. One day after Au(III) addition, *Eg*L 1 sample displays a unique and intense SPR band (Fig. 6a-1—D1 spectrum). The intensity of this SPR band seems to have already reached its maximum at this time as the spectra D3, D6, and D9, recorded, respectively, 3, 6, and 9 days after Au(III) introduction, look almost identical with D1 (Fig. 6a-1—D3, D6, D9 spectra). This is confirmed by the plateau obtained when the maximum of the absorbance versus time is plotted (Fig. 6a-2).

At first, the UV–Vis spectrum of *Eg*L 2 ($[Au^{3+}] = 10^{-4}$ M) does not present any SPR band a day after the introduction of Au(III) into *Eg*L 2 culture (Fig. 6b—D1 spectrum). Then, an SPR band, of a minor intensity, appears 2 days later (Fig. 6b—D3 spectrum). This band seems to vanish almost totally over time (D6 and D9 spectra of the same figure). This confirms why it was not possible to image the Au-NPs produced by this sample using TEM as the few produced nano-structured objects were likely either retained within the cells or surrounded by a vigorous and still-growing population of cells. This fact is in good agreement with the macroscopic aspect of this sample and with the evolution of the intensity of the chlorophyll a of this sample, pointing out that this amount of gold is not lethal. The viability and the growth of the cells explain the presence of other absorption bands in the same spectra (Fig. 6b) due most likely to the different photosynthetic pigments.

In the case of *Eg*M 1 ($[Au^{3+}] = 10^{-3}$ M), the intensity of the SPR band reaches its maximum a day after Au(III) addition (Fig. 6c—D1 spectrum) and then diminishes over time while slightly broadening

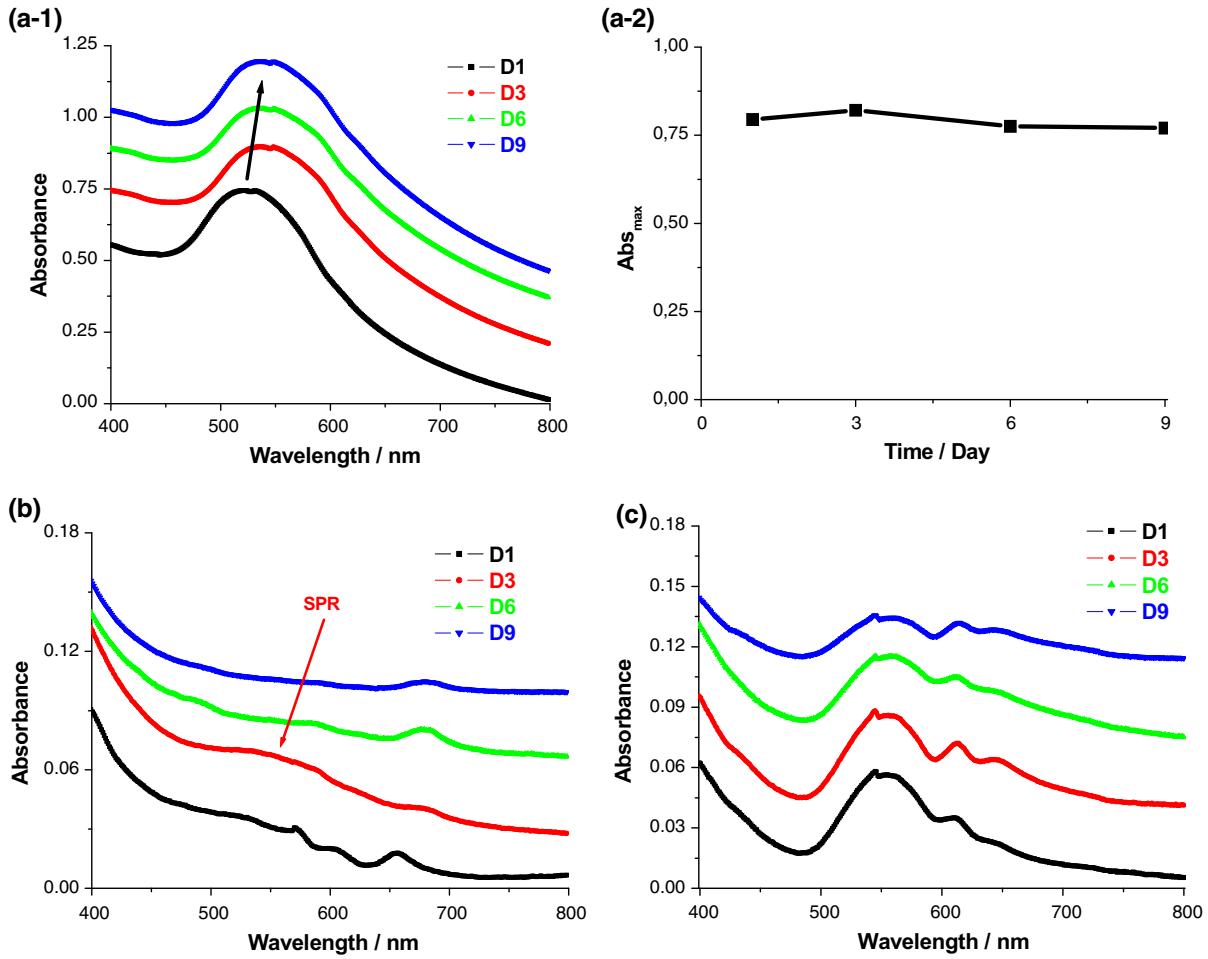

Fig. 6 Evolution over time of the SPR band of bioproduced Au-NPs by **a**-1 *Eg*L 1 ($[Au^{3+}] = 10^{-3}$ M), **b** *Eg*L 2 ($[Au^{3+}] = 10^{-4}$ M), and **c** *Eg*M 1 ($[Au^{3+}] = 10^{-3}$ M). **a**-2 Release kinetics of produced Au-NPS by *Eg*L 1. *Black arrow* in **a**-1 indicates a red-shift of the SPR band for Au-NPs picked from *Eg*L 1. *Red arrow* in **b** points out the vanishing SPR band of Au-NPs taken from *Eg*L 2

evidencing the aggregation and the sedimentation of the bioproduced Au-NPs (D3, D6, and D9 spectra of the same figure). As in the previous case, 2 other bands are persistent and are also most likely due to the photosynthetic pigments.

Regarding the release kinetics and the yield, several comments could be easily made: (i) The unique and well-defined band observed in UV–vis spectra (Fig. 6a-1) means that Au-NPs in majority are in spherical in shape. (ii) The SPR band plateauing 1 day after Au(III) introduction into *Eg*L 1 ($[Au^{3+}] = 10^{-3}$ M) indicates that the rate of Au-NPs production using *E. gracilis*, grown in L medium, is quite high (Fig. 6a-2) and higher than in the case of *K. flaccidum*, for instance, reported in a previous work (Dahoumane et al. 2012a) which displays a slower kinetics by accomplishing this task within several days after being challenged with the same amount of gold cations ($[Au^{3+}] = 10^{-3}$ M). (iii) Data gathered for the two species revealed that the yield of Au-NP biosynthesis is higher in the case of *Eg*L 1 compared to *K. flaccidum* (Dahoumane et al. 2012a). In fact, the SPR band intensity reaches ~0.75 in absorbance in the case of *Eg*L 1 versus ~0.6 in the case of *K. flaccidum* challenged with the same amount of Au(III) (10^{-3} M). (iv) The produced Au-NPs using cells of *E. gracilis* grown in L medium (*Eg*L 1, $[Au^{3+}] = 10^{-3}$ M) exhibit a better colloidal stability compared to Au-NPs

made by *E. gracilis* cells grown in M medium either at 10^{-3} M (*Eg*M 1, Fig. 6b) or 10^{-4} M of Au(III) (Dahoumane et al. 2014b). The fast kinetics and the high yield of Au-NP biosynthesis are due most likely to the fast rate of growth of *E. gracilis* cells when cultured in L medium making higher amounts of enzymatic machinery available to carry out the work; the better colloidal stability of the as-produced nanostructures is likely ensured by the remaining molecules of lactate which adsorb onto their surface. As a reminder, *E. gracilis* is not known to produce any exopolysaccharides (EPS). Moreover, the nature of the interaction between the lactate molecules and the Au-NPs has yet to be clarified. Au-NPs were only stable in the presence of lactate, and therefore, the presence of cell lysis components can be excluded from being the stabilizing agent. In fact, Au-NPs made using cells of *E. gracilis* grown in mineral medium (*Eg*M) lack colloidal stability even if the added gold cations, either at a concentration of 10^{-4} M (Dahoumane et al. 2014b) or 10^{-3} M (Figs. 1c, 6c), trigger each time a mass cell death.

The slight red-shift in the SPR band of $\sim$5 nm, indicated with a black arrow in Fig. 6a-1, may be linked mainly to the evolution in the composition of the surrounding medium of Au-NPs due to the release of large amounts of biomolecules, organic matter, and cell debris, triggered by the mass cell death following the introduction of Au(III) into the culture at a lethal dose (10^{-3} M). This fact was observed previously with other species even if it was not commented (Dahoumane et al. 2012a). Indeed, a deeper look at the kinetics of gold nanoparticle release by, for instance, *K. flaccidum* following the addition of tetrachloroauric acid at 10^{-3} M, or by *A. flos-aquae* following the addition of tetrachloroauric acid at 10^{-4} M (cf. Fig. 2a, e of Dahoumane et al. (2012a), respectively), reveals clearly the existence of the same phenomenon which could be easily correlated to the mass death of these two species as evidenced by the disappearance of the chlorophyll a fluorescence measured using PAM (pulse amplitude modulated) fluorimeter (cf. Fig. 9a, d of Dahoumane et al. (2012a), respectively). In addition to that, other factors may contribute to that minor red-shift, such a stronger interaction between the Au-NPs due to improved yield and bigger Au-NPs being produced starting from smaller ones synthesized inside the cells and released into culture medium where they might have undergone an increase in size by the reduction of gold cations at their surface.

Conclusion

This study demonstrates that the metabolism of living cells of *E. gracilis* microalga has an important impact on its ability to modulate the biosynthesis of gold nanoparticles. In fact, mixotrophic conditions, i.e., photosynthesis and a source of organic carbon, in other words, *E. gracilis* grown in L medium and allowed to perform photosynthesis as it is exposed to a photoperiod of 16-h light/8-h dark, induce a cell growth several times faster than when the cells are grown exclusively under autotrophic conditions, i.e., cells relying only on photosynthesis to grow. As a result, the kinetics of Au-NP biosynthesis become quicker and the yield higher due to the presence of larger amounts of living cells acting as nanofactories by internalizing Au(III) cations and reducing them to zero-valent gold (Au(0)), promoting therefore Au-NP production. Moreover, the colloidal stability of the as-produced nano-objects is significantly improved most likely due to the adsorption of remaining molecules of lactate onto the nanoparticle surface. These molecules are also probably responsible for the apparition of particular shapes among the population of Au-NPs. These findings add up to the amassed knowledge on the biosynthesis of inorganic nanoparticles using biological resources, in general, and living cells of microalgae, in particular, tackling key factors that govern such processes, therefore paving the way for the design of photobioreactors for the scalable and eco-friendly production of valuable nanomaterials.

Acknowledgments SAD thanks the French Ministry of Higher Education and Scientific Research for financial support.

Compliance with ethical standards

Conflict of interest The authors report no conflict of interest.

References

Azizi S, Ahmad MB, Namvar F, Mohamad R (2014) Green biosynthesis and characterization of zinc oxide nanoparticles using brown marine macroalga *Sargassum muticum* aqueous extract. Mater Lett 116:275–277. doi:10.1016/j.matlet.2013.11.038

Barwal I, Ranjan P, Kateriya S, Yadav SC (2011) Cellular oxido-reductive proteins of *Chlamydomonas reinhardtii* control the biosynthesis of silver nanoparticles. J Nanobiotechnol 9:56. doi:10.1186/1477-3155-9-56

Brayner R et al (2007) Cyanobacteria as bioreactors for the synthesis of Au, Ag, Pd, and Pt nanoparticles via an enzyme-mediated route. J Nanosci Nanotechnol 7:2696–2708. doi:10.1166/jnn.2007.600

Brayner R et al (2009) Photosynthetic microorganism-mediated synthesis of akaganeite (beta-FeOOH) nanorods. Langmuir 25:10062–10067. doi:10.1021/la9010345

Brayner R et al (2012) Intracellular biosynthesis of superparamagnetic 2-lines ferri-hydrite nanoparticles using *Euglena gracilis* microalgae. Colloid Surf B 93:20–23. doi:10.1016/j.colsurfb.2011.10.014

Castro L, Blazquez ML, Munoz JA, Gonzalez F, Ballester A (2013) Biological synthesis of metallic nanoparticles using algae. IET Nanobiotechnol 7:109–116. doi:10.1049/iet-nbt.2012.0041

Castro L, Blázquez ML, Muñoz JA, González F, Ballester A (2014) Mechanism and applications of metal nanoparticles prepared by bio-mediated process. Rev Adv Sci Eng 3:199–216. doi:10.1166/rase.2014.1064

Chakraborty N, Banerjee A, Lahiri S, Panda A, Ghosh AN, Pal R (2009) Biorecovery of gold using cyanobacteria and an eukaryotic alga with special reference to nanogold formation—a novel phenomenon. J Appl Phycol 21:145–152. doi:10.1007/s10811-008-9343-3

Dahoumane SA, Djédiat C, Yeprémian C, Couté A, Fiévet F, Brayner R (2010) Design of magnetic akaganeite-cyanobacteria hybrid biofilms. Thin Solid Films 518:5432–5436. doi:10.1016/j.tsf.2010.04.001

Dahoumane SA, Djediat C, Yéprémian C, Couté A, Fiévet F, Coradin T, Brayner R (2012a) Species selection for the design of gold nanobioreactor by photosynthetic organisms. J Nanopart Res 14:883. doi:10.1007/s11051-012-0883-8

Dahoumane SA, Djédiat C, Yeprémian C, Couté A, Fiévet F, Coradin T, Brayner R (2012b) Recycling and adaptation of *Klebsormidium flaccidum* microalgae for the sustained production of gold nanoparticles. Biotechnol Bioeng 109:284–288. doi:10.1002/bit.23276

Dahoumane SA, Wijesekera K, Filipe CD, Brennan JD (2014a) Stoichiometrically controlled production of bimetallic gold-silver alloy colloids using micro-alga cultures. J Colloid Interface Sci 416:67–72. doi:10.1016/j.jcis.2013.10.048

Dahoumane SA, Yéprémian C, Djédiat C, Couté A, Fiévet F, Coradin T, Brayner R (2014b) A Global approach of the mechanism involved in the biosynthesis of gold colloids using micro-algae. J Nanopart Res 16:2607. doi:10.1007/s11051-014-2607-8

Feurtet-Mazel A, Mornet S, Charron L, Mesmer-Dudons N, Maury-Brachet R, Baudrimont M (2015) Biosynthesis of gold nanoparticles by the living freshwater diatom *Eolimna minima*, a species developed in river biofilms. Environ Sci Pollut Res. doi:10.1007/s11356-015-4139-x

Focsan M, Ardelean II, Craciun C, Astilean S (2011) Interplay between gold nanoparticle biosynthesis and metabolic activity of cyanobacterium *Synechocystis* sp. PCC 6803. Nanotechnology. doi:10.1088/0957-4484/22/48/485101

Govindaraju K, Basha SK, Kumar VG, Singaravelu G (2008) Silver, gold and bimetallic nanoparticles production using single-cell protein (*Spirulina platensis*) Geitler. J Mater Sci 43:5115–5122. doi:10.1007/s10853-008-2745-4

Govindaraju K, Kiruthiga V, Kumar VG, Singaravelu G (2009) Extracellular synthesis of silver nanoparticles by a marine alga, *Sargassum Wightii* Grevilli and their antibacterial effects. J Nanosci Nanotechnol 9:5497–5501. doi:10.1166/jnn.2009.1199

Halvorson Lahr R, Vikesland PJ (2014) Surface-enhanced Raman spectroscopy (SERS) cellular imaging of intracellulary biosynthesized gold nanoparticles. ACS Sustain Chem Eng 2:1599–1608. doi:10.1021/sc500105n

Jeffryes C, Agathos SN, Rorrer G (2015) Biogenic nanomaterials from photosynthetic microorganisms. Curr Opin Biotechnol 33:23–31. doi:10.1016/j.copbio.2014.10.005

Jena J, Pradhan N, Nayak RR, Dash BP, Sukla LB, Panda PK, Mishra BK (2014) Microalga *Scenedesmus* sp.: a potential low-cost green machine for silver nanoparticle synthesis. J Microbiol Biotechnol 24:522–533. doi:10.4014/jmb.1306.06014

Kaduková J, Velgosová O, Mražíková A, Marcinčáková R (2014) The effect of culture age and initial silver concentration on biosynthesis of Ag nanoparticles. Nova Biotechnol Chim 13:28–37. doi:10.2478/nbec-2014-0004

Kannan RRR, Arumugam R, Ramya D, Manivannan K, Anantharaman P (2013a) Green synthesis of silver nanoparticles using marine macroalga *Chaetomorpha linum*. Appl Nanosci 3:229–233. doi:10.1007/s13204-012-0125-5

Kannan RRR, Stirk WA, Van Staden J (2013b) Synthesis of silver nanoparticles using the seaweed *Codium capitatum* P.C. Silva (Chlorophyceae). S Afr J Bot 86:1–4. doi:10.1016/j.sajb.2013.01.003

Klaus-Joerger T, Joerger R, Olsson E, Granqvist C-G (2001) Bacteria as workers in the living factory: metal-accumulating bacteria and their potential for materials science. Trend Biotechnol 19:15–20. doi:10.1016/S0167-7799(00)01514-6

Kumar P, Senthamil Selvi S, Govindaraju M (2012a) Seaweed-mediated biosynthesis of silver nanoparticles using *Gracilaria corticata* for its antifungal activity against *Candida* spp. Appl Nanosci 3:495–500. doi:10.1007/s13204-012-0151-3

Kumar P, Senthamil Selvi S, Lakshmi Prabha A, Prem Kumar K, Ganeshkumar S, Govindaraju M (2012b) Synthesis of silver nanoparticles from *Sargassum tenerrimum* and screening phytochemicals for its anti-bacterial activity. Nano Biomed Eng 4:12–16. doi:10.5101/nbe.v4i1.p12-16

Kumar P, Govindaraju M, Senthamilselvi S, Premkumar K (2013) Photocatalytic degradation of methyl orange dye using silver (Ag) nanoparticles synthesized from *Ulva lactuca*. Colloid Surf B 103:658–661. doi:10.1016/j.colsurfb.2012.11.022

Lengke MF, Fleet ME, Southam G (2006a) Morphology of gold nanoparticles synthesized by filamentous cyanobacteria from gold(I)-thiosulfate and gold(III)-chloride complexes. Langmuir 22:2780–2787. doi:10.1021/la052652c

Lengke MF, Fleet ME, Southam G (2006b) Synthesis of platinum nanoparticles by reaction of filamentous cyanobacteria with platinum(IV)-chloride complex. Langmuir 22:7318–7323. doi:10.1021/la060873s

Lengke MF, Fleet ME, Southam G (2007a) Biosynthesis of silver nanoparticles by filamentous cyanobacteria from a silver(I) nitrate complex. Langmuir 23:2694–2699. doi:10.1021/la0613124

Lengke MF, Fleet ME, Southam G (2007b) Synthesis of palladium nanoparticles by reaction of filamentous cyanobacterial biomass with a palladium(II) chloride complex. Langmuir 23:8982–8987. doi:10.1021/la7012446

Li Y et al (2015) Biosynthesis of silver nanoparticles using *Euglena gracilis*, *Euglena intermedia* and their extract. IET Nanobiotechnol 9:19–26. doi:10.1049/iet-nbt.2013.0062

Liu B, Xie J, Lee JY, Ting YP, Chen JP (2005) Optimization of high-yield biological synthesis of single-crystalline gold nanoplates. J Phys Chem B 109:15256–15263. doi:10.1021/jp051449n

Luangpipat T, Beattie IR, Chisti Y, Haverkamp RG (2011) Gold nanoparticles produced in a microalga. J Nanopart Res 13:6439–6445. doi:10.1007/s11051-011-0397-9

Mahdavi M, Namvar F, Ahmad MB, Mohamad R (2013) Green biosynthesis and characterization of magnetic iron oxide (Fe_3O_4) nanoparticles using seaweed (*Sargassum muticum*) aqueous extract. Molecules 18:5954–5964. doi:10.3390/molecules18055954

Mahdieh M, Zolanvari A, Azimee AS, Mahdieh M (2012) Green biosynthesis of silver nanoparticles by *Spirulina platensis*. Sci Ira F 19:926–929. doi:10.1016/j.scient.2012.01.010

Mata YN, Torres E, Blazquez ML, Ballester A, Gonzalez F, Munoz JA (2009) Gold(III) biosorption and bioreduction with the brown alga *Fucus vesiculosus*. J Hazard Mater 166:612–618. doi:10.1016/j.jhazmat.2008.11.064

Mohseniazar M, Barin M, Zarredar H, Alizadeh S, Shanehbandi D (2011) Potential of microalgae and lactobacilli in biosynthesis of silver nanoparticles. BioImpacts 1:149–152. doi:10.5681/bi.2011.020

Momeni S, Nabipour I (2015) A simple green synthesis of palladium nanoparticles with *Sargassum* alga and their electrocatalytic activities towards hydrogen peroxide. Appl Biochem Biotechnol 176:1937–1949. doi:10.1007/s12010-015-1690-3

MubarakAli D, Gopinath V, Rameshbabu N, Thajuddin N (2012) Synthesis and characterization of CdS nanoparticles using C-phycoerythrin from the marine cyanobacteria. Mater Lett 74:8–11. doi:10.1016/j.matlet.2012.01.026

Nagarajan S, Arumugam Kuppusamy K (2013) Extracellular synthesis of zinc oxide nanoparticles using seaweeds of Gulf of Mannar, India. J Nanobiotechnol 11:39. doi:10.1186/1477-3155-11-39

Ninfa AJ, Ballou DP, Benore M (2010) Fundamental laboratory approches for biochemistry and biotechnology, 2nd edn. Wiley, Hoboken

Pandimurugan R, Thambidurai S (2014) Seaweed-ZnO composite for better antibacterial properties. J Appl Polym Sci 131:40948. doi:10.1002/app.40948

Pantidos N, Horsfall LE (2014) Biological synthesis of metallic nanoparticles by bacteria, fungi and plants. J Nanomed Nanotechnol 5:5. doi:10.4172/2157-7439.1000233

Parial D, Patra HK, Dasgupta AKR, Pal R (2012a) Screening of different algae for green synthesis of gold nanoparticles. Eur J Phycol 47:22–29. doi:10.1080/09670262.2011.653406

Parial D, Patra HK, Roychoudhury P, Dasgupta AK, Pal R (2012b) Gold nanorod production by cyanobacteria—a green chemistry approach. J Appl Phycol 24:55–60. doi:10.1007/s10811-010-9645-0

Patel V, Berthold D, Puranik P, Gantar M (2015) Screening of cyanobacteria and microalgae for their ability to synthesize silver nanoparticles with antibacterial activity. Biotechnol Rep 5:112–119. doi:10.1016/j.btre.2014.12.001

Rahman A, Ismail A, Jumbianti D, Magdalena S, Sudrajat H (2009) Synthesis of copper oxide nano particles by using *Phormidium* Cyanobacterium. Indo J Chem 9:355–360

Rajeshkumar S, Malarkodi C, Gnanajobitha G, Paulkumar K, Vanaja M, Kannan C, Annadurai G (2013) Seaweed-mediated synthesis of gold nanoparticles using *Turbinaria conoides* and its characterization. J Nanostruct Chem 3:44. doi:10.1186/2193-8865-3-44

Rösken LM, Körsten S, Fischer CB, Schönleber A, van Smaalen S, Geimer S, Wehner S (2014) Time-dependent growth of crystalline Au-nanoparticles in cyanobacteria as self-reproducing bioreactors: 1. Anabaena sp. J Nanopart Res 16:2370. doi:10.1007/s11051-014-2370-x

Satapathy S, Shukla SP, Sandeep KP, Singh AR, Sharma N (2014) Evaluation of the performance of an algal bioreactor for silver nanoparticle production. J Appl Phycol 27:285–291. doi:10.1007/s10811-014-0311-9

Schröfel A, Kratošová G, Bohunická M, Dobročka E, Vávra I (2011) Biosynthesis of gold nanoparticles using diatoms-silica-gold and EPS-gold bionanocomposite formation. J Nanopart Res 13:3207–3216. doi:10.1007/s11051-011-0221-6

Senapati S, Syed A, Moeez S, Kumar A, Ahmad A (2012) Intracellular synthesis of gold nanoparticles using alga *Tetraselmis kochinensis*. Mater Lett 79:116–118. doi:10.1016/j.matlet.2012.04.009

Sharma B, Purkayastha DD, Hazra S, Gogoi L, Bhattacharjee CR, Ghosh NN, Rout J (2014) Biosynthesis of gold nanoparticles using a freshwater green alga, *Prasiola crispa*. Mater Lett 116:94–97. doi:10.1016/j.matlet.2013.10.107

Stein JR (1973) Handbook of phycological methods. Culture methods and growth measurements. Cambridge University Press, Cambridge

Subramaniyam V, Subashchandrabose SR, Thavamani P, Megharaj M, Chen Z, Naidu R (2015) *Chlorococcum* sp. MM11—a novel phyco-nanofactory for the synthesis of iron nanoparticles. J Appl Phycol 27:1861–1869. doi:10.1007/s10811-014-0492-2

Xie J, Lee JY, Wang DIC, Ting YP (2007a) Identification of active biomolecules in the high-yield synthesis of single-crystalline gold nanoplates in algal solutions. Small 3:672–682. doi:10.1002/smll.200600612

Xie J, Lee JY, Wang DIC, Ting YP (2007b) Silver nanoplates: from biological to biomimetic synthesis. ACS Nano 1:429–439. doi:10.1021/nn7000883

Yin X, Chen S, Wu A (2010) Green chemistry synthesis of gold nanoparticles using lactic acid as a reducing agent. Micro Nano Lett 5:270–273. doi:10.1049/mnl.2010.0117